

Optical diffraction on fractals

C. Allain and M. Cloitre

Laboratoire d'Hydrodynamique et Mécanique Physique, Ecole Supérieure de Physique et de Chimie Industrielles de la Ville de Paris, 10 rue Vauquelin, 75231 Paris Cedex 05, France

(Received 8 July 1985; revised manuscript received 15 October 1985)

Diffraction experiments are performed on two-dimensional deterministic fractals such as Cantor bars or Vicsek fractals. We show that the intensity $I(\mathbf{q})$ which is scattered at a wave vector \mathbf{q} by a fractal grating is simply its optical Fourier transform. This allows a direct determination of the Hausdorff dimension D and of other geometrical characteristics of fractals. Applications of this analog method to experimentally obtained aggregates are discussed.

Most of the fractals obtained in real experimental situations are self-similar objects, i.e., their geometrical characteristics are invariant over scale dilatations. They are characterized by the fractal dimension D which measures the manner in which the mass M , embedded in a sphere of radius R , increases: $M(R) \cong R^D$. Similarly, the density-density correlation function $g(R)$ conforms to a power-law variation: $g(R) \cong R^{D-d}$ (d is the Euclidean space dimension). Experimentally obtained fractals are usually analyzed through this mass-radius relation or the two-point correlation function. Current procedures consist of taking photographs of the objects under study, recording these pictures in a computer through an image processing device, and finally calculating $M(R)$ or $g(R)$. It is also possible to have access to D when studying the variation of the intensity $I(q)$ scattered by a fractal at a wave vector \mathbf{q} : $I(q) \cong q^{-D}$.¹ This relation has been used to interpret small-angle scattering experiments on silica gels² or colloids.³

In this paper, we present diffraction experiments on deterministic fractal gratings. In particular, we are interested in one- and two-dimensional self-similar fractals which are constructed recursively. For instance, Cantor triadic bars⁴ are obtained by dividing a bar into three equal segments and removing its middle third. Then the same construction rule is applied to the two remaining parts and so on; the fractal dimension of this fractal is $\ln 2 / \ln 3$. The fractal of Fig. 1(b) has been introduced recently by Vicsek as a two-dimensional model for imitating diffusion-controlled deposition on a surface.⁵ The first cell, which consists of five squares, is repeated according to its original configuration *ad infinitum*. These fractals are generated on a microcomputer and drawn on a precision graphics plotter HP 7470. Finally, they are photographed using a high-resolution 24–35-mm film (for instance, a Kodak Infocapture AHU 1454 film allows a resolving power up to 500 lines/mm).

A first limitation arises from the A4 format of our graphics plotter and from the minimum width of the lines which can be drawn (0.2 mm). Consequently, the ratio between the largest scale L and the smallest one ϵ is about $L/\epsilon \cong 10^3$. For instance, in the special case of triadic Cantor bars or Vicsek fractals, as the factor of division at each iteration is 3, we are limited to objects obtained from 7 iterations. This restriction is released if we use a more efficient graphics plotter, or if we are interested in experimen-

tally obtained fractals. In these cases, the limitations arise from the finite size of an elementary grain on the film, which defines the smallest scale which can be recorded on the film (here $\epsilon_{\min} \cong 2 \mu\text{m}$), and from its size L which determines the resolution of $I(q)$ measurements. Thus, the ratio L/ϵ , which gives the number of scales which may be recorded on such a film is $L/\epsilon \cong 10^4$. In practice, most of the fractals encountered in experimental situations have a smaller number of scales and can be recorded by this way.

The optical arrangement on which the diffraction experiments were performed is represented in Fig. 2. The beam La of an argon laser ($\lambda = 488 \text{ nm}$, 600 mW) is expanded by a microscope lens 1; at its focal point, a small pinhole (25 μm in diameter) acts as a spatial filter selecting the transverse mode TE_{00} . L is a converging lens (Nikkor 690 mm, $f = 11$). We assume that its aperture is smaller than

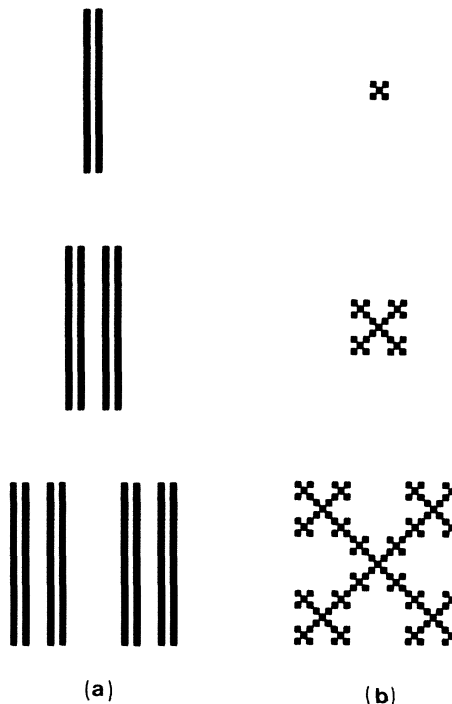


FIG. 1. Successive stages of generating iterative fractals: (a) Cantor bars, (b) Vicsek fractals.

that of the expanded beam so that it can be considered totally and uniformly illuminated. Moreover, in the following we shall neglect any diffraction effect which might be introduced by lens L . The fractal grating G to be studied is disposed between lens L and screen S .

Let us now demonstrate that the diffraction pattern observed on screen S is the optical Fourier transform (OFT) of the grating. G is illuminated by a spherical wave which converges on the screen, S . G and S being separated by a distance d , the amplitude of this spherical wave just before the grating is

$$a(x,y) = a_0 \exp\left[-\frac{j\pi}{\lambda d}(x^2 + y^2)\right]. \quad (1)$$

In the plane of the grating, this amplitude takes a new value,

$$a'(x,y) = a(x,y)T(x,y), \quad (2)$$

where $T(x,y)$ denotes the transmittance function of the grating. On S , the amplitude diffracted by G is given by the Fresnel's diffraction formula:⁶

$$A(u,v) = \frac{A_0}{j\lambda d} \exp\left[\frac{j\pi}{\lambda d}(u^2 + v^2)\right] \int \int_{-\infty}^{+\infty} a'(x,y) \exp\left[\frac{j\pi}{\lambda d}(x^2 + y^2)\right] \exp\left[-\frac{2j\pi}{\lambda d}(ux + vy)\right] dx dy. \quad (3)$$

Now replacing $a'(x,y)$ in (3) by its value given by (1) and (2), one sees that the quadratic term $\exp[j\pi(x^2 + y^2)/\lambda d]$ which appears in (3) vanishes. Finally, the amplitude of the diffraction pattern of G can be written simply as follows:

$$A(p,q) = \frac{A_0}{j\lambda d} \exp[j\pi\lambda d(p^2 + q^2)] \int \int_{-\infty}^{+\infty} T(x,y) \exp[-2j\pi(px + qy)] dx dy. \quad (4)$$

where $p = u/\lambda d$ and $q = v/\lambda d$ are spatial frequencies. Apart from the fact that a phase term $\exp[j\pi\lambda d(p^2 + q^2)]$ takes place in the prefactor of the integral in (4), $A(p,q)$ is the Fourier transform of the transmittance $T(x,y)$ of G . Varying the distance d between the grating and the screen, we can continuously change the magnification ratio of the diffraction pattern. As far as we use a quadratic detector, such as a photomultiplier, which records the energy diffracted at (p,q) , we measure the square of the Fourier transform of $T(x,y)$. In Fig. 2, this photomultiplier PM is connected to a multichannel analyzer which records $I(p,q)$. A high-precision motorized micrometer controls the displacement of the photomultiplier and performs a precise scanning of the Fourier plane. In our experiment, a translation of 10 mm corresponds to a variation in the diffraction angle equal to 0.28 deg. A small pinhole (25 μm) ensures the selection of the wave vector (p,q) . The uncertainty in the determination of the diffraction angle, due to the aperture of the pinhole, is about 10^{-2} deg.

Let us now calculate analytically the OFT of Cantor bars. The optical transmittance of the grating at iteration n , $T_n(x,y)$, is determined recursively from $T_0(x,y)$. In effect, at iteration 0 the grating reduces to a single bar of width $\epsilon = 1$, centered at point $x = 0$; its transmittance is $T_0(x) = \text{rect}(\epsilon = 1, x = 0)$, where $\text{rect}(\epsilon, x)$ is a rectangle function of width ϵ at point x . At the first iteration, the transmittance $T_1(x)$ is expressed as a function of $T_0(x)$:

$$T_1(x) = T_0(x) * \delta(x - 1) + T_0(x) * \delta(x + 1),$$

where $*$ denotes a convolution operator and $\delta(x - x_0)$ a Dirac function at $x = x_0$. Since the way of generating Cantor bars is iterative, it is easy to establish that a similar rela-

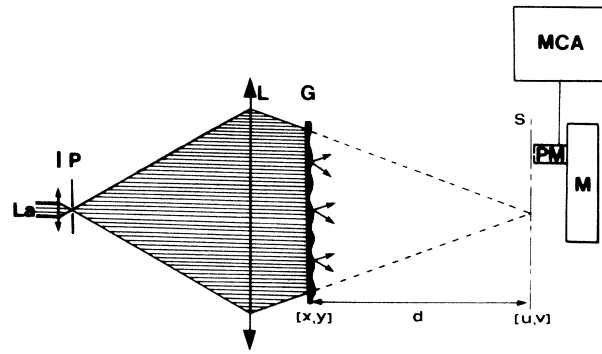


FIG. 2. Schematic showing the experimental arrangement. La, argon laser; l, microscope lens; P, spatial filter; L, Fourier transform lens; G, fractal grating; PM, photomultiplier; MCA, multichannel analyzer; M, motorized micrometer.

tion exists at any stage n between T_n and T_{n-1} :

$$T_n(x) = T_{n-1}(x) * \delta(x - 3^{n-1}) + T_{n-1}(x) * \delta(x + 3^{n-1}).$$

Taking the Fourier transform of the two sides of this relation,

$$A_n(q) = [2 \cos(2\pi 3^{n-1} q)] A_{n-1}(q).$$

Finally, the amplitude scattered by Cantor bars at iteration n is

$$A_n(q) = 2^n \left(\prod_{i=0}^{n-1} \cos(2\pi 3^i q) \right) A_0(q); \quad A_0(q) = \frac{\sin \pi q}{\pi q}.$$

$A_0(q)$ is the amplitude diffracted by a single bar. We deduce from $A_n(q)$ the intensity diffracted in the Fourier plane:

$$I_n(q) = 2^{2n} \left(\prod_{i=0}^{n-1} \cos(2\pi 3^i q) \right)^2 \left(\frac{\sin \pi q}{\pi q} \right)^2.$$

As usual in diffraction experiments, $I_n(q)$ includes a form factor $F(q)$ and a structure factor. The form factor corresponds to the intensity scattered by an elementary unit, here a bar of width ϵ ,

$$F(q) = \left(\frac{\sin \pi q}{\pi q} \right)^2.$$

The structure factor $S_n(q)$ reveals the way in which the elementary units are distributed in the fractal. It is given by the series

$$S_n(q) = 2^{2n} \left(\prod_{i=0}^{n-1} \cos(2\pi 3^i q) \right)^2.$$

The coefficient $S_n(0) = 2^{2n}$ is equal to N^2 , where $N = 2^n$ is the number of diffracting elements. The mass of a single bar has been taken equal to 1 and $S_n(0)$ can be interpreted as the square of the total mass M . Thus, experimentally, M is simply measured by $I_n(0)$. In the following, we have normalized $S_n(0)$ to 1.

Let us investigate more deeply the properties of $S_n(q)$. First, the whole spectra can be deduced completely from the range $q = (0, 0.25)$ by symmetry operations about $q = 0.25$ and $q = 0.50$; this is a consequence of the regular properties of Cantor bars. In Fig. 3, we have calculated and plotted the structure factors S_5, S_6 , and S_7 . Clearly, as n increases, these spectra are composed of an increasing number of frequency bands B_j , which are scale invariant over dilatations of factor 3. For a fractal obtained at iteration n , we can define $n - 1$ frequency bands B_j , each of them extending in the range $(0.25/3^j, 0.25/3^{j-1})$, j varying from 1 to $n - 1$. The spectral density of $S_n(q)$ over a frequency band B_j is defined by

$$\langle S_n(q) \rangle = \frac{3}{2q} \int_{q/3}^q S_n(w) dw \quad (5)$$

In Fig. 5, we have calculated and plotted $\langle S_7(q) \rangle$ over each band B_j . We find that it varies according to the power law

$$\langle S_n(q) \rangle = q^{-D} \quad (6)$$

where D is the fractal dimension ($D = \ln 2 / \ln 3$). This relation, obtained after an averaging operation in order to break up any regularity due to the deterministic properties of Cantor bars, is the same as the one expected for random fractals.¹ It results from the self-similarity of Cantor bars.

Experimental and calculated spectra of Cantor triadic bars are compared in Fig. 4 ($n = 7$). Here, the resolving power, Δ , which measures the capacity of separating two wave vectors is proportional to $1/L$: $\Delta \cong 2.85 \times 10^{-5} \mu\text{m}^{-1}$. The

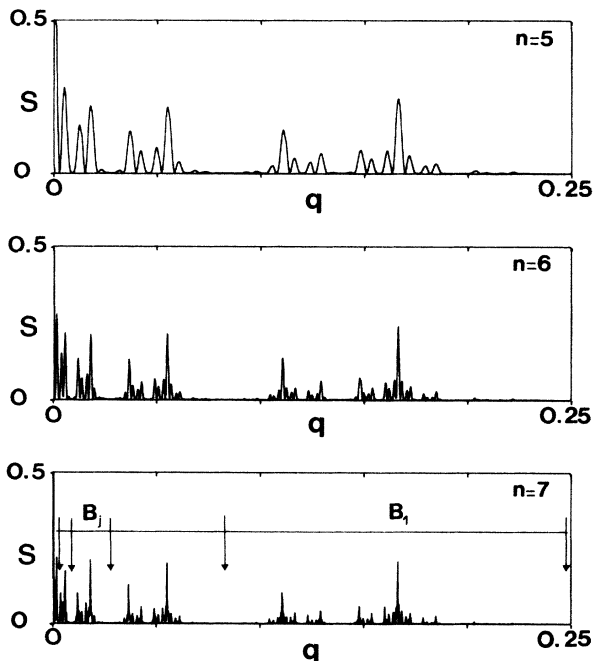


FIG. 3. Structure factors of Cantor bars obtained for $n = 5, 6$, and 7 .

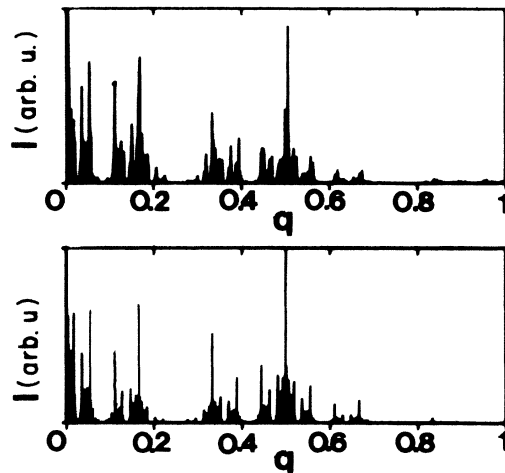


FIG. 4. Comparison between the calculated diffraction spectrum of Cantor bars (up) and the experimental data (down); $n = 7$.

largest spatial frequency ($0.065 \mu\text{m}^{-1}$), which is associated with the smallest scale ϵ of G , has been normalized for convenience to $q = 1$. The first zero of the form factor $F(q)$ occurs for $q = 1$; thus, at high spatial frequencies, $F(q)$ smears out the structure of the grating. On the contrary, at low angles ($q < 0.25$), $F(q) \cong 1$, and $I_n(q) \cong S_n(q)$. We have calculated $\langle S_7(q) \rangle$ according to formula (5) for the experimental spectra. The resulting data are presented in Fig. 5; at very low angles the experimental data cannot be used, since they are affected by the contribution of a central peak due to the incident beam. The calculated value of D fits with the expected one within an uncertainty of 10%; this includes the reproducibility of the experiments. This large uncertainty is due to the small number of iterations used to construct the fractal which has been studied.

The preceding method can be generalized to any deterministic or random fractal in two dimensions. The experimental procedure is applied identically with the proviso that

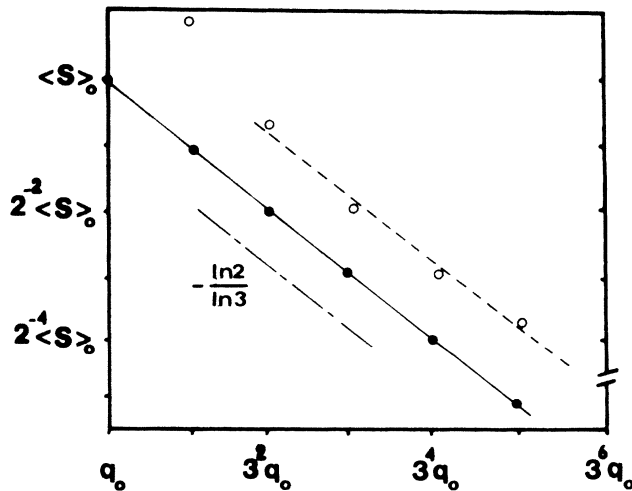


FIG. 5. Log-log plot giving the variations of $\langle S_7(q) \rangle$ for Cantor bars. The curves showing the calculated data (●) and the experimental results (○) have been shifted for clarity.

a two-dimensional (2D) scanning of the Fourier plane is necessary to record $I_n(p, q)$ completely. Figure 6 shows the calculated structure factor $S_5(p, q)$ of a Vicsek fractal ($n=5$) and its OFT. They clearly exhibit invariance over dilatations of factor 3. As above, at high spatial frequencies, the structure of the grating is smeared out by the form factor, i.e., the diffraction pattern of a square of side ϵ . We have checked that the diffracted intensity averaged over each of the frequency bands, which are scale invariant, varies according to the power-law variation (6).

Summarizing, we have presented an analog method for performing OFT of 2D fractal gratings. The diffraction patterns possess the same symmetry properties as the objects in real space; they exhibit self-similarity because of the fractal nature of the gratings. Applications to 1D Cantorian triadic bars have been described in detail; we have compared the experimental spectra to the exact one, obtained from analytical calculations. In particular, we have shown that the method enables a direct determination of L , ϵ , and D . Extensions to 2D deterministic fractals have been discussed briefly; further applications to random 2D structures are now in progress in order to investigate experimentally obtained fractals.

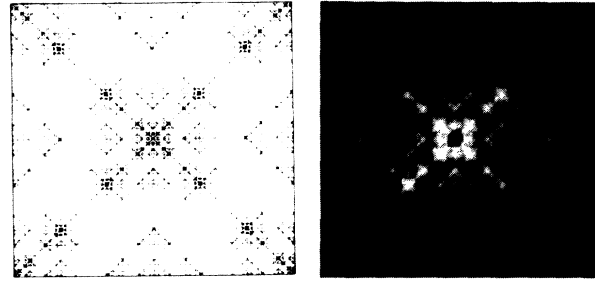


FIG. 6. Structure factor of a Vicsek fractal ($n=5$) and its experimental diffraction pattern.

We are indebted to P. Evesque and J. C. Charmet, who gave us enlightening suggestions concerning the calculation of Fourier transforms of fractals. This work is supported by an ATP from the Centre National de la Recherche Scientifique (CNRS), France. The Laboratoire d'Hydrodynamique et Mécanique Physique is "Unité Associé au CNRS No. 857."

¹T. A. Witten and L. M. Sander, *Phys. Rev. B* **27**, 5686 (1983).

²D. W. Shaefer and K. D. Keefer, *Phys. Rev. Lett.* **53**, 1383 (1984).

³D. W. Shaefer, J. E. Martin, D. Cannel, and P. Wiltzius, *Phys. Rev. Lett.* **52**, 2371 (1984).

⁴B. B. Mandelbrot, *The Fractal Geometry of Nature* (Freeman, New

York, 1982), Chap. 8.

⁵T. Vicsek, *J. Phys. A* **16**, L647 (1983).

⁶J. W. Goodman, *Introduction à l'optique de Fourier et à l'holographie* (Masson, Paris, 1982), p. 78.

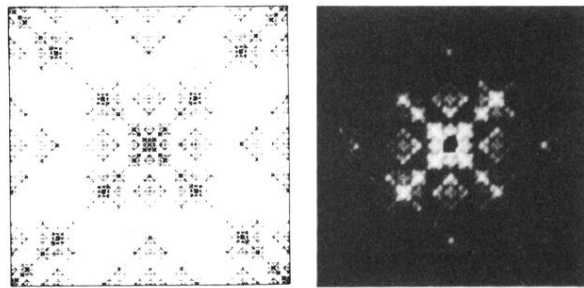


FIG. 6. Structure factor of a Vicsek fractal ($n = 5$) and its experimental diffraction pattern.